Sensors & Transducers, Vol. 160, Issue 12, December 2013, pp. 635-644

www.sensorsportal.com

Sensors & Transducers

© 2013 by IFSA

http://www.sensorsportal.com

An Image Acquiring Method for Position and Attitude Measurement of High-Speed Target in Wind Tunnel

Wei LIU, Shuangjun LIU, Yang ZHANG, Zhiliang SHANG, Xin MA

Laboratory for Precision and Non-traditional Machining Technology of Ministry of Education,
Dalian University of Technology,
116024, PR China
Tel.: +86-0411-84708159, fax: +86-0411-84708159
E-mail: lw2007@dlut.edu.cn

Received: 14 October 2013 /Accepted: 22 November 2013 /Published: 30 December 2013

Abstract: In order to measure the position and attitude of the target in wind tunnel experiment, a co-operation target image acquiring method is proposed for high-speed targets by utilizing principles of the machine vision and the optimization of lighting source. Base on the CCD model, the effect of the characteristics of the camera, light source and the co-operation target on the image quality is analyzed firstly. Then, the signal-to-noise ratio between co-operation target and background is employed to detect the image quality of high-speed targets. The distribution rules of spatial brightness and SNR image of micro glass beads reflective material marker are derived for monocular camera and binocular camera. Finally, experimental results indicate that the image acquiring method presented is effective for measuring the position and attitude of high-speed target in the wind tunnel experiment. *Copyright © 2013 IFSA.*

Keywords: High-speed targets, Image acquiring, Co-operation, Machine vision, Position and attitude.

1. Introduction

The aircraft store-dropping is in the interference flow field during the early period of leaving the aircraft, its position and attitude are vital to ensure the security of the aircraft [1]. The main methods of researching aircraft store separation characteristics are conducted in the wind tunnel, with scaling down the aircraft store to keep the geometric similarity of the model and material object. However, in the wind tunnel experiments, it is difficult to accurately measure the position and attitude of aircraft store-dropping, due to the dark environment and the high speed of store-dropping.

Usually, the methods of measuring the position and attitude are mainly differential GPS method [2], inertial element-based measurement method, the Star camera, sun sensor, photoelectric theodolite, machine vision method and so on [3]. More attentions has been attracted by machine vision measurement method for the measurement of the position and attitude of the aircraft store-dropping in the wind tunnel store-dropping experiments, due to its advantages of non-contact measurement, high accuracy, fast processing speed, high security and good repeatability, etc. Northern Digital Inc. produced a measurement system of the position and attitude named OptotrakTM [4], which is composed of three accurately calibrated linear CCD. The system can capture the self-luminous MARKER point and get each MARKER point in 3D space coordinates at different time. The precision of the system can achieve 0.1 mm RMS, and the resolution can reach 0.01 mm. However, the highest frequency of data

sampling is 250 Hz which is difficult to satisfy the requirement of the high-speed target measurement. In addition, ONERA utilized a binocular visual system to measure wing deformations [5]. They provided a feasible deformation method, named Onera Deformation Model Measurement based on visual principle. This system could collect the images of high-speed targets under dark condition of wind tunnel by comparison with the characteristics of the black and white for the extraction of feature points. However, in the high-speed wind tunnel, the brightness and brightness uniformity of integral space is low. Black and white information is hard to distinguish and the system will produce a large noise. In addition, multiple exposure techniques and high-speed photographic techniques are employed to capture for the image of dropping stores in the wind tunnel experiments. However, the image quality is difficult to guarantee, due to the unclear contour of the dropping stores, directly captured by the high-speed camera system. Moreover, in the image processing, feature extraction are mostly based on the gray scale characteristics or contour characteristics [6]. Furthermore, the gray change of rotational dropping stores on the surface is not clear, the contour angle point information is very limited, which easily lead to a follow-up dealing difficulty after directly capturing the images. Thus, the image acquiring method of high-speed target in wind tunnel experiment is very necessary to detect the position and attitude of the aircraft dropping stores.

In this paper, a co-operation target image acquiring method is proposed for high-speed targets based on machine vision technology. Base on the CCD model, the effect of characteristics of the camera, light source and co-operation target on the image quality is analyzed firstly. Then, the image acquiring system is fabricated. Moreover, the signal-to-noise ratio between co-operation target and background is employed to detect the image quality of high-speed targets. The distribution rules of spatial brightness and signal-to-noise ratio are derived for monocular camera and binocular camera. Finally, experiments are carried out to evaluate the performance of the proposed method.

2. Image Acquiring Method and System for High-Speed Targets

2.1. CCD Photosensitive Imaging Model

Usually, the CCD of the photoelectric conversion characteristics can be expressed as [7]:

$$y = aH^{\gamma} + b, \tag{1}$$

where y is the output signal voltage (V), H is the exposure $(lx \cdot s)$, and a is the slope of a straight line which represents the response of the CCD $(V / lx \cdot s)$, γ is the photoelectric conversion coefficient $(\gamma \approx 1)$, and b is the CCD output voltage without illumination, which is called dark output voltage (V). When the amount of exposure is certain, the size of a has a direct effect on the amplitude of the output of the CCD. Moreover, a CCD sensor in good conditions should have a high optical responsivity and a low dark output voltage, and there is the relation of $aH^{\gamma} >> b$ under normal circumstances. Exposure H can be represented by:

$$H = \int\int E(\lambda,t)\eta_s(\lambda)d\lambda dt, \tag{2}$$

where $\eta_s(\lambda)$ is the photosensitive efficiency of the CCD, a function of wavelength λ, $E(\lambda,t)$ is the illumination changing with the wavelength λ and the time t. $E(\lambda,t)$ can be expressed as $E(\lambda)$ during the shooting scene when the exposure time is shorter, and the time impact for the illumination is ignored. Thus the exposure can be expressed as:

$$H = t \cdot \int E(\lambda)\eta_s(\lambda)d\lambda, \tag{3}$$

However, $\eta_s(\lambda)$ is the nature of the camera system, and cannot be changed for a CCD. Moreover, t is a fixed value under the fixed shutter speed of the high-speed imaging, so the exposure H mainly depends on the illumination $E(\lambda)$ caused by measured targets on the CCD sensor. When the relative positions between the targets which will be measured by the camera are relatively fixed, its value is mainly determined by the intensity of the radiation of the target. The intensity of the reflection of the target is mainly depends on the reflectance of the intensity of the radiation of the illumination light source and the reflectance of the target, and also is affected by the illumination angle and the shooting angle. To simplify the model, only a particular wavelength of light waves is studied, which results form that for different wavelength of light waves, the CCD sensitivity, lens transmission coefficient, and the surface reflectance are different. Supposed that micro element on the measuring surface is written by ds, radiant energy from the target surface reflection captured by lens can be written as:

$$\Phi_o = \Phi_i(I) \cdot \rho(\theta,\varphi,\eta), \tag{4}$$

where $\Phi_i(I)$ is the radiant flux formed on the micro-surface ds corresponding to the light source; when the relative position of the light source is determined, $\Phi_i(I)$ is a linear function of the light intensity I; $\rho(\theta,\varphi,\eta)$ is the correlation coefficient between the radiation energy captured by lens and incident radiation energy, which is a function of the angle θ, shooting angle φ and the reflectance of the surface

of the target η. During shooting, which corresponds to a particular moment, the positional relationship of the micro-surface element ds, the camera, and the light source is determined. Thus, θ and φ are constants. $\rho(\theta,\varphi,\eta)$ is an approximate linear function of η, and can be simplified by:

$$\Phi_o = \Phi_i(I)\cdot\rho(\eta), \quad (5)$$

Reflection illumination of camera photosensitive member by the infinitesimal element ds can be approximately expressed as:

$$E = \Phi_o/(\pi\cdot r^2)\cdot\alpha, \quad (6)$$

where r is the radius of the lens and α is the transmission coefficient of the lens, which are both fixed value decided by the lens. According to Equation (5) and (6), the relative position among camera, light source, and the micro-surface element ds at a particular moment in the shooting process is fixed, illumination suffered from the photosensitive elements of the CCD is uniquely determined by the intensity of light source I and the reflectivity of the target η. According to Equation (1) and (3), at any particular moment, the signal response of the imaging surface element ds of CCD, which can also be interpreted as the corresponding gray scale of ds without image gain, exhibits an approximately proportional relationship with the light intensity I and the reflectance η:

$$y\infty(\eta, I), \quad (7)$$

2.2. Image Acquiring Method

During the wind tunnel experiments on measuring the position and attitude of high-speed targets, there are some problems of image acquiring to be resolved as following: (a) poor lighting conditions due to narrow and small installation space for light sources; (b) low surface reflectivity of high-speed targets; (c) high illumination uniformity need for whole measuring range. Thus, in this paper, a co-operation target image acquiring method is proposed for high-speed targets by virtue of high-speed cameras. Firstly, co-operation marker with high reflectivity is employed to extract the position and attitude information of high-speed targets. Then, the position of light source and high-speed camera are optimized for obtaining high illumination uniformity. Finally, clear image can be captured by adjusting the parameters of light source and high-speed camera. Fig. 1 shows the schematic of image acquiring method for measuring the position and attitude of high-speed targets in wind tunnel. In addition, the signal-to-noise ratio between co-operation target and background is proposed to access the image quality of high-speed targets [8, 9].

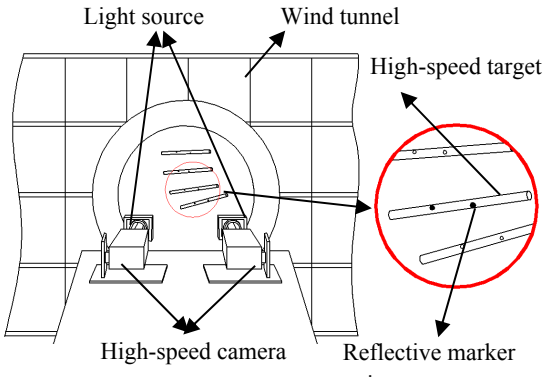

Fig. 1. The schematic of image acquiring method for measuring the position and attitude of high-speed targets.

As shown in Fig. 1, retro-reflection marker with the micro-glass bead material is selected as the co-operation marker, which can reflect lots of light projected on the surface of the retro-reflection material to the camera. Furthermore, the constant current diffused LED light is selected to illuminate the measured targets, which can avoid space brightness fluctuations over time in the high-speed shooting. Smallest angle between the reflected light and incident light on the micro-glass bead material can give the brightest reflected lights, which requires the LED source close to the lens as far as possible. Thus, a design of arranging the quadrate shape constant current LED to surround symmetrically the lens, is employed in this paper, to increase light collection capabilities of camera, and to facilitate light intensity distribute more evenly.

2.3. Image Acquiring System

The image acquiring system for measuring the position and attitude of high-speed targets, as shown in Fig. 2, consists of two high-speed cameras (Photron SA-X) with 17-35m lens (Nikon), two low-angle light sources with quadrate shape (CCS – FPQ2-120SW), vibration isolated table, two sets of high-precision electronic control platform, and one computer. Two low-angle lighting sources are arranged rounding the lens of two cameras, respectively. Two low-angle lighting sources are arranged rounding the lens of two cameras, respectively. Two electronic control platforms are used to install cameras, and change their positions and angles for calibrating the parameters of cameras. In addition, in order to abate the vibration in wind tunnel experiments, the measurement system is fixed on the vibration isolated table, as shown in Fig. 2.

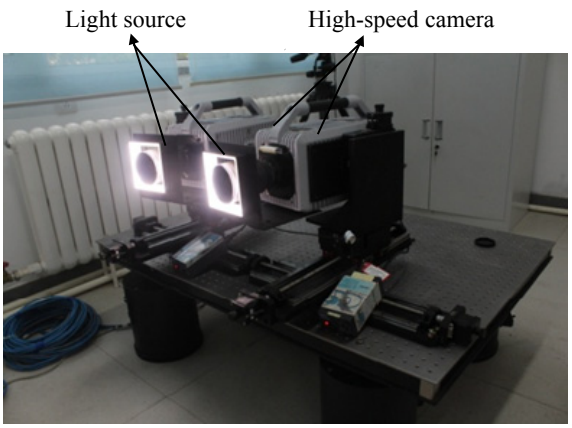

Fig. 2. Image acquiring system for position and attitude measurement of high-speed targets.

3. SNR of Image of High-Speed Targets

As mentioned above, due to the complicated shape of the LED light source, it is difficult to accurately know how the reflective material reflection intensity, illumination intensity in whole measured space. However, the reflective properties and brightness distribution of the material in measuring space is important to image quality of high-speed targets, which affect directly the precision and robustness of position and attitude measuring system. Therefore, in this paper, an access method of image based on SNR is proposed to detect the image quality in whole measuring space.

3.1. SNR of Image

In this paper, the strong background noise in the environment is substitute by white paper, and the SNR of image is defined by [10]:

$$SNR = \frac{G_R^B}{G_N^B}, \tag{8}$$

where G_R^B is the gray corresponding to the brightness of the reflective material, G_N^B is the gray corresponding to the brightness of the background in the environment. Moreover, G_R^B and G_N^B are function of (x, y), which are pixels in the image. As shown in Fig. 3 (a) and Fig. 3 (b), the spatial brightness distribution of micro glass beads material covered on a plane (Fig. 3 (a)) is illustrated within the pixels of 1024×1024, where the plane is perpendicular to the lens with a distance from high speed camera of 880 mm in a dark condition at the shooting speed of 5000 frames per second.

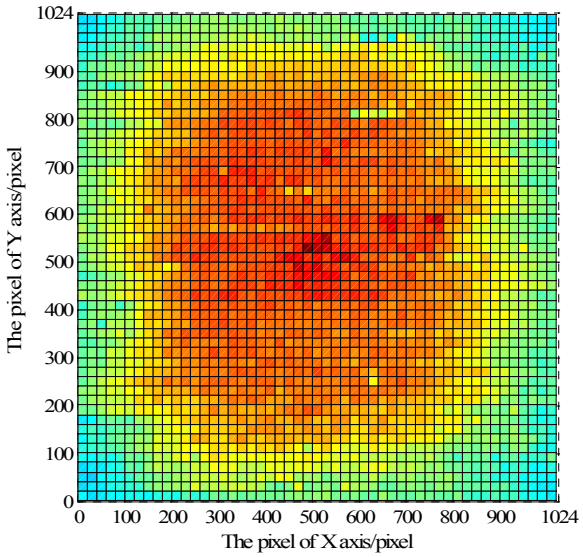

(a) The brightness distribution

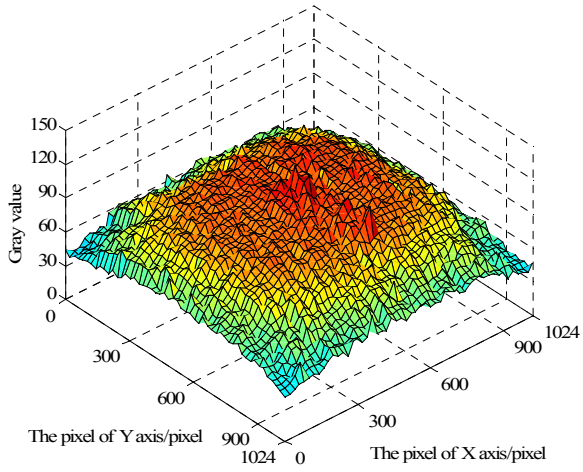

(b) 3D map of brightness distribution

Fig. 3. Spatial brightness distribution of micro glass beads material.

The reflective material brightness distribution is affected by the shape of the LED light source and the property of reflective material. As shown in Fig. 3 (b), the brightest place is in the center of the image plane, and owing to the non-uniformity brightness of light source, a relatively bright square area appears around the center of plane. With increasing the distance from the center of the image plane, the brightness will scale down gradually, and the variation range of gray value is relatively wide (100-180), which presents challenge for capturing clear image. Fig. 4 shows spatial brightness distribution of white paper, which is selected to substitute the strong background noise in the environment. Fig. 5 illustrates the SNR distribution of image of micro glass beads material plane, where the distance from the lens of camera is 800 mm, and a square-shaped LED light source is arranged surround symmetrically the lens. Similarly,

the SNR of image is varied by brightness change of micro glass beads with the variation range of 4-10.

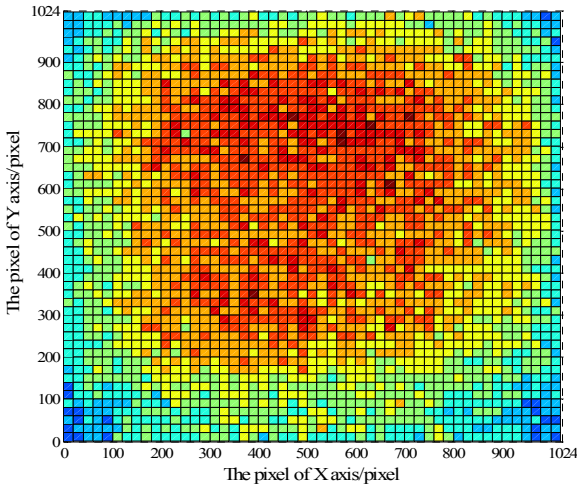

(a) The brightness distribution of white paper

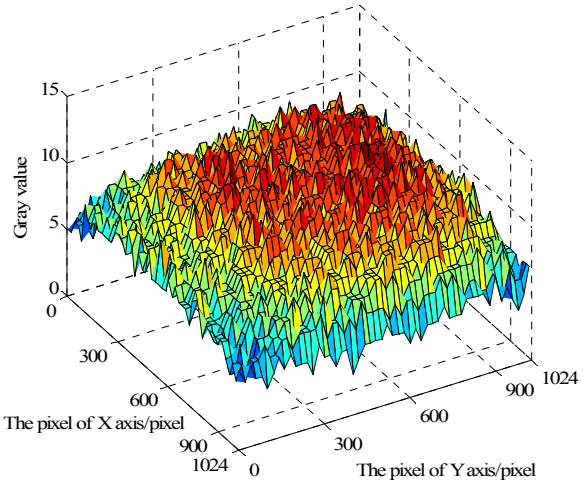

(b) 3D map of brightness distribution of white paper.

Fig. 4. Spatial brightness distribution of white paper.

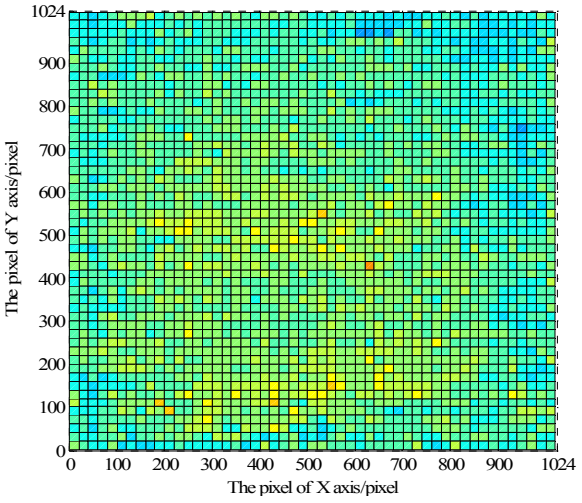

Fig. 5 (a). Distribution of the space plane SNR.

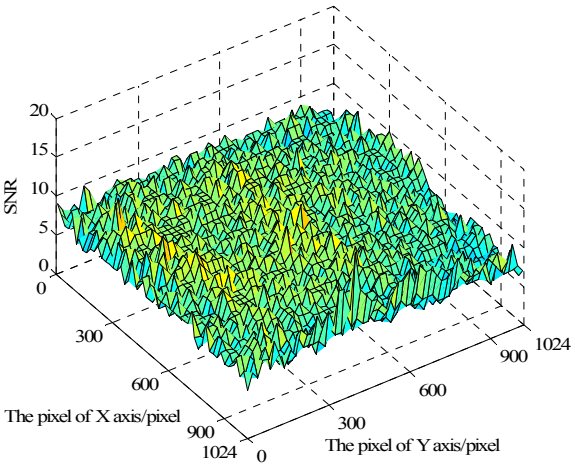

Fig. 5 (b). 3D distribution map of the space plane SNR.

In addition, the brightness distribution of micro glass beads in a space is detected in this paper. Through paralleled shifting the reflective plane of micro glass beads within the distance from the camera lens of 660 mm-880 mm, and capturing the image every 20 mm, we can obtain the SNR changing rule and brightness distribution of the micro glass beads in the measurement space of (650 mm×650 mm×220 mm). As shown in Table 1, when the distance from plane to lens ranges from 880 mm to 660 mm, the SNR varies from 6 to 10, which is suitable to extracting the feature of image in the process of measuring position and attitude of high-speed targets.

Table 1. The brightness and SNR distribution of space micro glass bead material.

No.	The distance to the camera /mm	Average SNR	Plane image grayscale average of micro glass bead material
1.	660	5.9492	154.0183
2.	680	6.2959	152.3761
3.	700	6.6392	150.8319
4.	720	6.9582	148.4669
5.	740	7.1948	146.9406
6.	760	7.4363	145.4373
7.	780	7.8569	144.1886
8.	800	8.3057	142.7307
9.	820	8.6297	140.5994
10.	840	8.9997	139.045
11.	860	9.3506	137.2865
12.	880	9.7436	135.9981

3.2. The Effect of Binocular Light Source on Image Acquiring

In order to measure the position and attitude of high-speed targets, two high-speed cameras and two light sources are employed in this paper. Since two

light sources have different effects on binocular cameras installed symmetrically, the SNR of different spatial location and image brightness distribution of micro glass bead reflective material should be discussed in this paper. Fig. 6 (a) shows the brightness effect of right light source on the left camera, Fig. 6 (b) shows the brightness effect of left light source on the right camera. Since the left light source is close to the right camera under narrow wind tunnel measurement space, the right camera system could acquire not only the brightness of the right light but also the some brightness of the left light. The brightness of the left light could affect the brightness and the SNR distribution acquired by the right camera system. Similarly, the right light source also affects the left camera system.

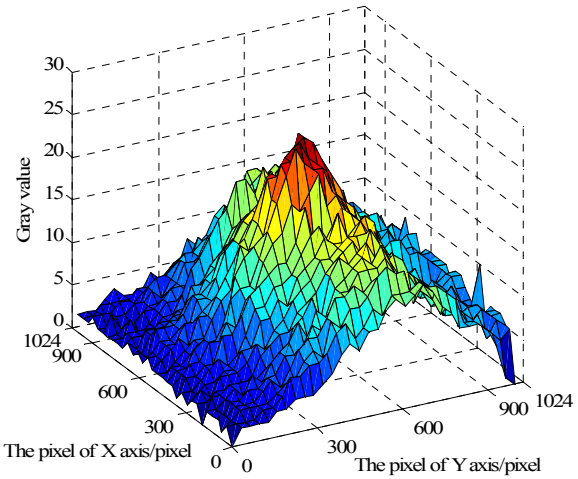

(a) The brightness of the right light on the left camera.

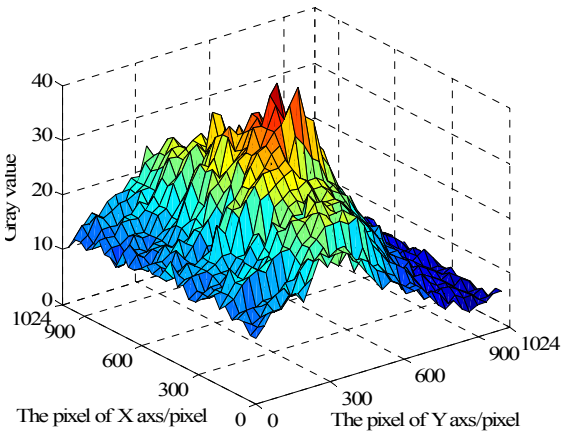

(b) The brightness of the left light on the right camera

Fig. 6. Distribution map of the space plane SNR.

Since the incoming light of retro reflective materials is returned by the original, the light of the closer the distance has a greater influence on the brightness of the light material markers. Fig. 7 shows SNR distribution of right light affecting on right camera is more uniform compared the left light affecting on the right camera.

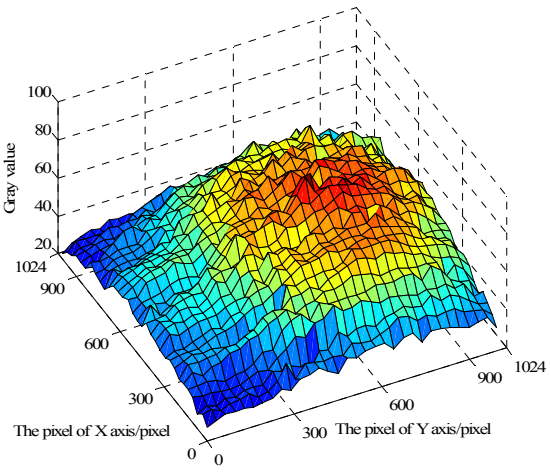

(a) The brightness of the left light on the left camera.

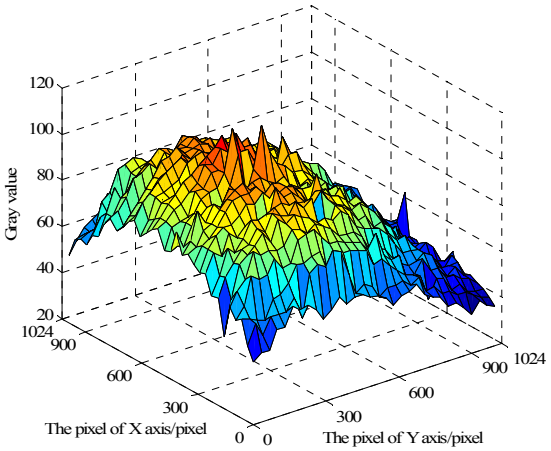

(b) The brightness of the right light on the right camera

Fig. 7. Distribution map of the space plane SNR.

As shown in Fig. 8 and Fig. 9, the brightness of retro reflective materials changes within the grey value of 100-200, and the SNR of image can reach the range of from 4 to 6, which can match the requirement of measuring position and attitude of high-speed targets.

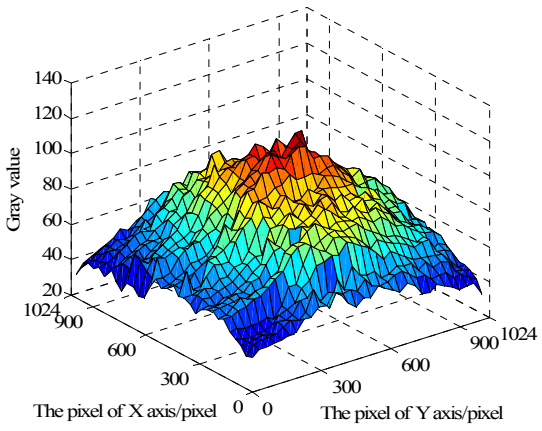

Fig. 8 (a). The brightness of the left and right light on the left camera.

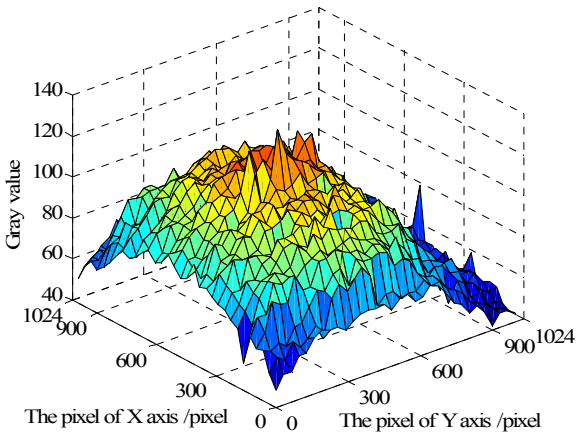

Fig. 8 (b). The brightness of the left and right light on the right camera.

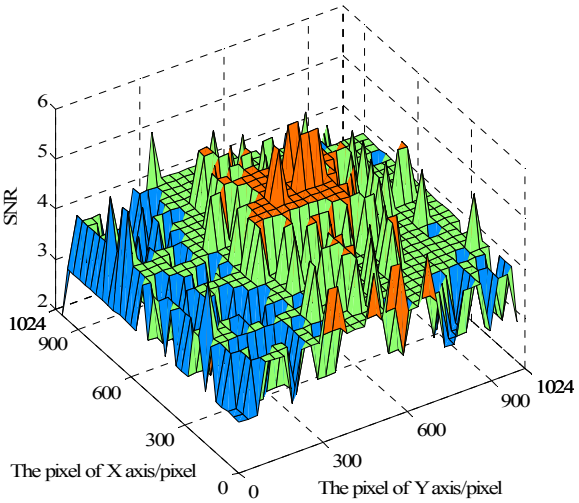

Fig. 9 (a). The left and right light on the left camera SNR

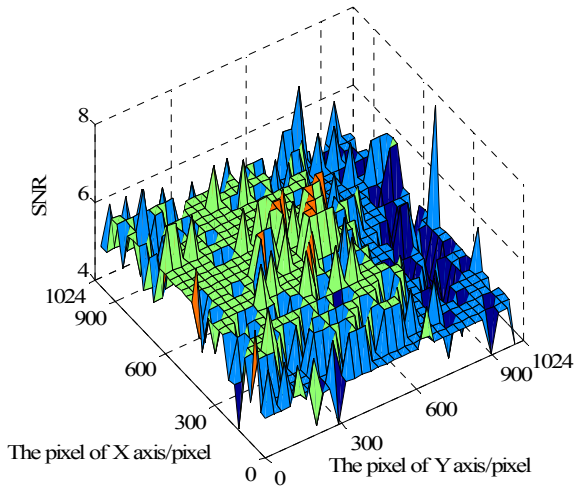

Fig. 9 (b). The left and right light on the right camera SNR.

3.3. SNR Distribution with Angular Changing

When the high-speed targets move in wind tunnel, its position and attitude varies indefinitely. Therefore, the SNR of co-operation marker with reflective material is discussed under different shooting angles. Experiments on image capturing of reflective material target are performed, and the average gray value of targets are recorded, as shown in Fig. 10, by rotating reflective material plane to change the angle between its surface and the camera. Since the incident angle of light source is the same with the camera-shooting angle, only the incident angle, representing that of both light source and camera, is to be discussed with the measured surface angle [11].

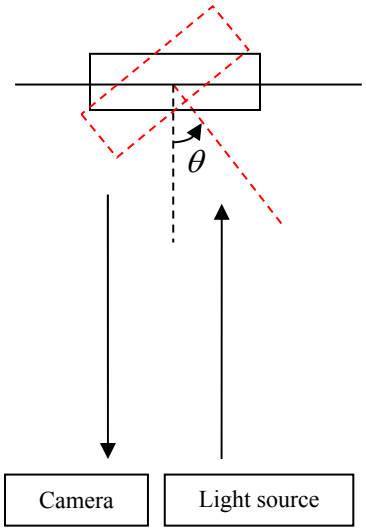

Fig. 10. Material reflective characteristics comparative experiment.

The specific experiment process is as follows: the simulated target surface is rotated continuously by 5° each time, with ranging from -80° to 80°. Under different incident angle, the experimental gray response results of both reflective material target and white paper are shown below in Fig. 11.

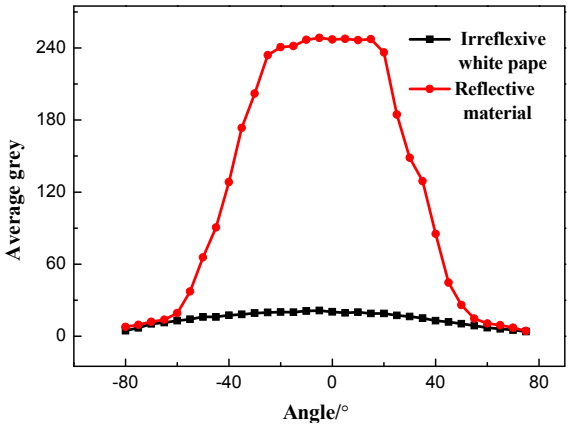

Fig. 11. Comparative experiment of material reflective properties.

As shown in Fig. 11, the reflective material has strong and stable reflective property, and gray response of its image keeps more than 200 when the incident angle ranges from -30° to 30°; its reflectivity decreases with absolute value of incidence angle increasing, however, it is still higher than the reflection effect of white paper, when the incident angle varying within the interval of (-70°, -30°) and (30°, 70°); its reflectivity is similar to white paper when the incident angle changes within the interval of (-80°, -70°) and (70°, 80°). Meanwhile, the reflectivity of white paper increases a little with the absolute value of incident angle increasing, however its range is smaller. Thus, this kind of micro glass bead reflective material on target can still guarantee high brightness, when angle of incidence is large.

4. The Dynamic Test of Target in Simulation

In order to validate the proposed image acquiring methods for measuring the position and attitude of high-speed target in the actual movement process, shooting measurement experiments of particle and flat targets are conducted in this paper.

4.1. Gravity Acceleration Measurement Experiment of Particle Target

For testifying the proposed method, gravity acceleration measurement experiment of particles with no initial velocity was conducted, under the circumstances of space brightness changing. In order to guarantee the target with no deflection during the dropping process and to make it easy to mark and arrange, the target is fabricated by a cube with covered a co-operation marker, as shown in Fig. 12. By capturing the target points by left and right high-speed cameras, the shooting results are listed in Fig. 13. The vertical displacement of particle in the world coordinate system was measured and the result is illustrated in Fig. 14.

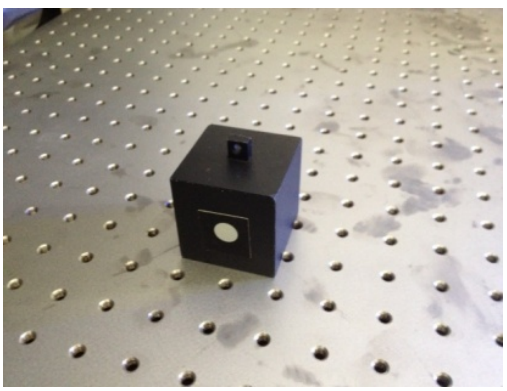

Fig. 12. Cube model.

(a) Left image (b) Right image

Fig. 13. Planar pattern boards for acquiring the point matches.

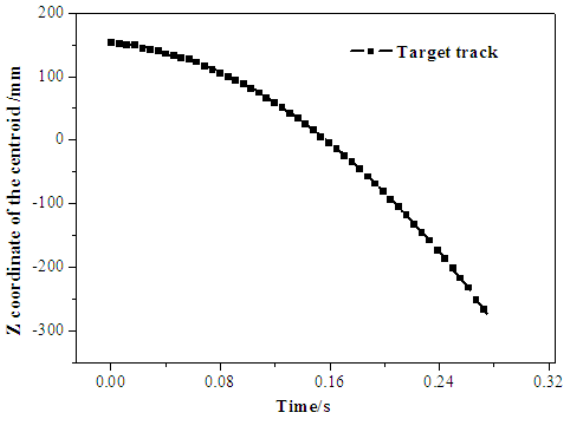

Fig. 14. The coordinate graph of target trajectory in gravity experiment results.

According to the theory of Newtonian mechanics, the vertical displacement of a target in gravity can be expressed as:

$$S = \frac{1}{2}gt^2 + v_0 t + S_0 , \tag{9}$$

where g is the acceleration of gravity, v_0 is the initial velocity of the object, S_0 is the object's initial position, t is the time. The experimental results in Fig. 14 are fitted by the equation of motion:

$$S = -4.8664t^2 - 0.2151t + 0.1564 , \tag{10}$$

It can be seen that the acceleration of gravity measured is $9.7327 m/s^2$, and the acceleration of gravity in Dalian region is $9.8011 m/s^2$, the measurement error of the acceleration of gravity is $0.0684 m/s^2$.

4.2. Measurement Experiment of Small Dropping Plane Targets

In order to measure the position and attitude of small plane target in the dropping process, the design of simulated object is shown in Fig. 15. By applying this image acquiring method in shooting

measurement of dropping small plane targets, the measured displacement result and axial angle measurement result of simulated target are shown in Fig. 16 and Fig. 17, respectively.

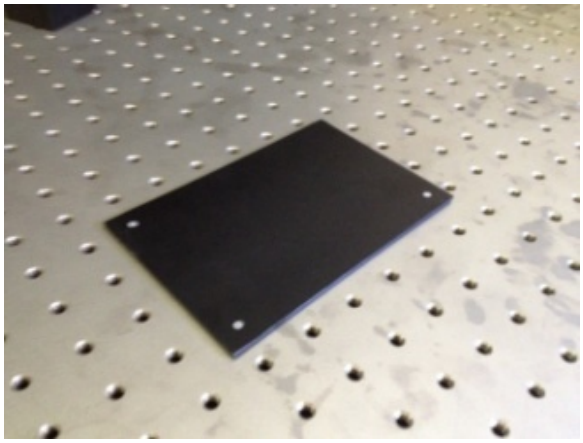

Fig. 15. Plane model for dynamic experiment.

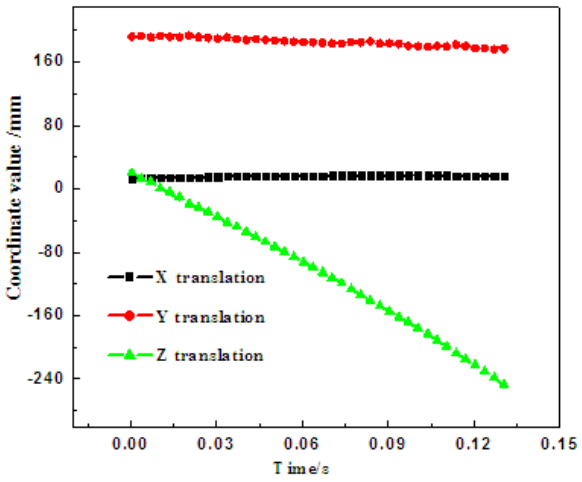

Fig. 16. The coordinate graph of simulated target with small plane attitude measurements results.

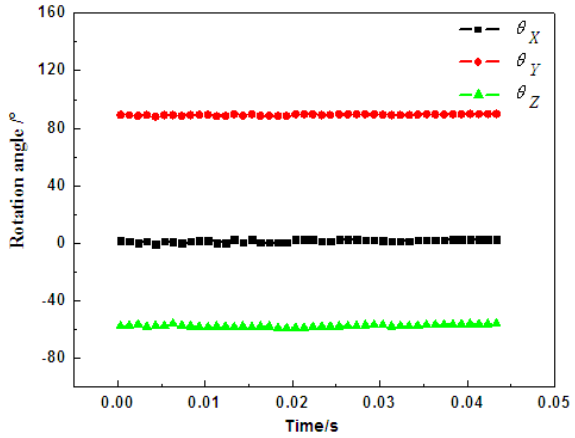

Fig. 17. The coordinate graph of simulated target with small plane attitude measurements results.

As shown in Fig. 16, displacements in X and Y direction of the dropping simulated target with zero initial velocity, remains the same, while Z direction displacement is like a quadratic curve under the acceleration of gravity. During the dropping process, the angular rotation θ_X , θ_Y and θ_Z of the target are kept basically 0°, 90°and -60°, which is similar to initial dropping result. Consequently, according to the two experiments above, the proposed image acquiring method is effective for measuring the position and attitude of high-speed target.

6. Conclusions

In this paper, a co-operation target image acquiring method is proposed for high-speed targets based on machine vision technology. Low-angle illumination light source, micro-glass bead reflective material marker, and high-speed camera are selected to fabricate the image acquiring system. Moreover, the signal-to-noise ratio between co-operation target and background is presented to detect the image quality of high-speed targets. The SNR of image micro glass beads reflective material marker for monocular camera can reach 10 for the measurement space of 650 mm × 650 mm × 220 mm, while the SNR can still reach 6 for binocular camera. Experimental results of dropping particle and flat targets without initial velocity indicate that the presented method is effective for measuring the position and attitude of high-speed targets in wind tunnel experiments.

Acknowledgements

This paper is supported by National Natural Science Foundation of China under Grant No. 51375075 and No. 51227004, the National Basic Research Program of China 973 Project under Grant No. 2014CB046504, and the Fundamental Research Funds for the Central Universities of China.

References

[1]. V. I. Shalaev, A. V. Fedorov, Dynamics of slender bodies separating from rectangular cavities, in *Proceedings of the AIAA Fluid Dynamics Conference & Exhibit,* Anaheim, CA, 11-14 June 2001, pp. 517-525.

[2]. M. Bryson, S. Sukkarieh, A comparison of feature and pose-based mapping using vision, inertial and GPS on a UAV, in *Proceedings of the Intelligent Robots and Systems (IROS)*, 2011, pp. 4256–4262.

[3]. Zhu Yongguo, Huang Xiang, Trajectory planning algorithm based on quaternion for 6-DOF aircraft wing automatic position and pose adjustment method, *Chinese Journal of Aeronautics*, Vol. 23, Issue 6, December 2010, pp. 707–714.

[4]. R. L. Watzlavick, J. P. Crowder, Comparison of model attitude systems – Active target photogrammetry, precision accelerometer, and laser interferometer, in *Proceedings of the AIAA, Advanced Measurement and Ground Testing Technology Conference*, New Orleans, LA, June 17-20, 1996, pp. 96-2252.

[5]. Y. Le Sant, A. Mignosi, Model deformation measurement (MDM) at Onera, in *Proceedings of the AIAA Applied Aerodynamics Conference*, Miami, FL, 25-28 June 2007.

[6]. Glauco V. Pedrosa, Marcos A. Batista, Image feature descriptor based on shape salience points, *Neurocomputing*, Vol. 120, 23 November 2013, pp. 156-163.

[7]. Yuanxing He, Xinyang Li, Error analysis of laser beam quality measured with CCD sensor and choice of the optimal threshold, *Optics & Laser Technology*, Vol. 45, February 2013, pp. 671–677.

[8]. Lichuan Gui, Tracking an aerodynamic model in a wind tunnel with a stereo high-speed imaging system, in *Proceedings of the Image and Signal Processing (CISP),* Yantai, 16-18 October 2010, pp. 1533-1537.

[9]. S. Srinivasan, R. Righetti, Trade-offs between the axial resolution and the signal-to-noise ratio in elastography, *Ultrasound in Medicine & Biology*, Vol. 29, Issue 6, June 2003, pp. 847–866.

[10]. Dominik Paul, Maxim Zaitsev, Improved SNR in linear reordered 2D bSSFP imaging using variable flip angles, *Magnetic Resonance Imaging*, Vol. 27, Issue 7, September 2009, pp. 933–941.

[11]. T. Grosges, Retro-reflection of glass beads for traffic road stripe paints, *Optical Materials*, Vol. 30, Issue 10, June 2008, pp. 1549–1554.

2013 Copyright ©, International Frequency Sensor Association (IFSA). All rights reserved.
(http://www.sensorsportal.com)